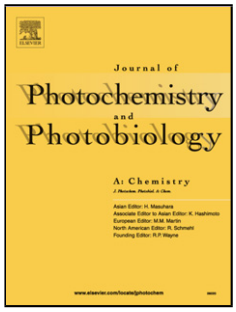

Title: Solvent and Substituent Effect on the Photophysical Properties of Pyrazoline Derivatives: A Spectroscopic Study

Authors: Ebru Bozkurt, Halise Inci Gul, Ebru Mete

PII: S1010-6030(17)31279-0
DOI: https://doi.org/10.1016/j.jphotochem.2017.10.010
Reference: JPC 10934

To appear in: *Journal of Photochemistry and Photobiology A: Chemistry*

Received date: 30-8-2017
Revised date: 30-9-2017
Accepted date: 7-10-2017

Please cite this article as: Ebru Bozkurt, Halise Inci Gul, Ebru Mete, Solvent and Substituent Effect on the Photophysical Properties of Pyrazoline Derivatives: A Spectroscopic Study, Journal of Photochemistry and Photobiology A: Chemistry https://doi.org/10.1016/j.jphotochem.2017.10.010

Solvent and Substituent Effect on the Photophysical Properties of Pyrazoline Derivatives: A Spectroscopic Study

Ebru Bozkurt[a*], Halise Inci Gul[b], Ebru Mete[c]

[a]*Program of Occupational Health and Safety, Erzurum Vocational Training School, Ataturk University, 25240 Erzurum, Turkey*
[b]*Department of Pharmaceutical Chemistry, Faculty of Pharmacy, Ataturk University, 25240 Erzurum, Turkey*
[c]*Department of Chemistry, Faculty of Science, Ataturk University, TR-25240 Erzurum, Turkey*
*Corresponding Author. Tel: +90(442)231 2667; Fax #: +90(442)231 2503

e-mail: ebrubozkurt@atauni.edu.tr (Ebru Bozkurt)

GRAPHICAL ABSTRACT

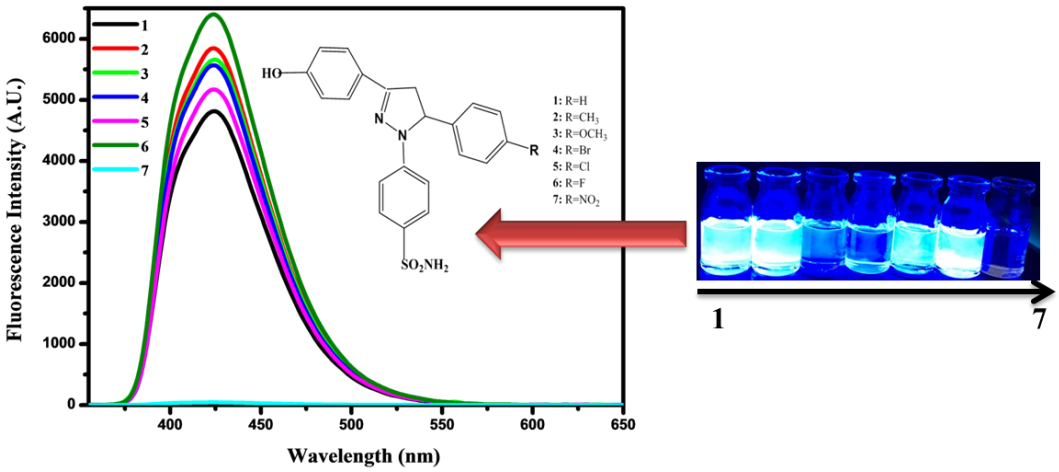

Highlights

- Seven pyrazoline derivatives (compound 1-7) were synthesized and their photo-physical properties were investigated.
- The effect of solvent and substituent on the photo-physical properties of new pyrazoline derivatives was determined.
- It suggested that the photo-physical properties of these biologically active novel molecular probes may be useful in some areas, such as labeling, sensor applications in different environments.

ABSTRACT

Pyrazoline derivatives are among solvatochromic dyes and they are the most widely used in many fields such as sensors, labeling agent and optoelectronic devices. Therefore, synthesis of new pyrazoline derivatives and determination of their optical behavior in different solvents are a very important research area. In this study, the solvatochromic behaviors of seven new synthetic pyrazoline derivatives, (4-[3-(4-Hydroxyphenyl)-5-aryl-4,5-dihydro-pyrazol-1-yl]benzenesulfonamides, compound **1-7**), were determined in different solvents. As a result of the measurements, a large red shifts in the fluorescence spectra of the compounds studied were observed for each compound, when the polarity of the solvent increased. Kamlet-Taft and Catalan parameters were used to describe the solvent-soluble interactions. The obtained results showed that the solvatochromic behavior of the compounds is dependent on their solvent polarity as well as the effect of the hydrogen-bonding properties of the solvents. It was also found that the increases in the polarity of the solvent was facilitated the non-radiative transition. Furthermore, the changes in the dipole moments of compounds **1-7** in different solvents at room temperature were calculated by using the Lippert–Mataga equation. It was very impressive that calculated fluorescence quantum yield values of the compounds studied here by using different solvents were remarkably high than the ones reported in the literatures for pyrazolines. In addition, the effect of substituent on the photo-physical properties of the compounds was also investigated. It was observed that the fluorescence intensity of the substituted compounds **2-6** increased comparing to the compound **1,** which is a non-substituted derivative. These changes were not dependent on electronic nature of the substituent on phenyl ring (i.e. electron donating and electron withdrawing substituent). According to data obtained it can be stated that these novel solvatochromic dyes studied here can be find application in pharmaceutical industry, as labeling agent, sensor applications as biosensors or analytical sensors and/or optoelectronic devices.

Keywords: Pyrazoline; Absorption; Fluorescence; Solvent effect; Kamlet-Taft and Catalan parameters

1. Introduction

Synthesis and the photo-physical characterization of new fluorogenic probes provide important contributions to many fields such as analytical, biochemical and optoelectronic [1-7]. Especially, solvatochromic fluorescent dyes have been extensively studied due to their potential applications as polarity-sensitive molecular probes. Several the optical properties of solvatochromic dyes (SD) such as the fluorescence intensity, color, the fluorescence quantum yield or lifetime are sensitive to the solvent medium in which SD are solved. The properties of SD lead their uses in several chemical, biological events in addition to their finding application in multimolecular systems as labeling agent, sensor ext. [8]. Pyrazoline derivatives are a widely used solvatochromic dye [9, 10]. Pyrazoline is a five-membered heterocyclic ring containing two nitrogen atoms can be considered as the best examples of this type of probes among fluorogenic probes. These type of compounds show strong fluorescence property due to conjugation available between pyrazoline and two phenyl rings. Pyrazolines and their complexes are also used in organic electroluminescent devices (OLEDs) due to high fluorescence quantum yield and strong fluorescence properties [11-16]. Furthermore, these compounds also have importance in medicinal chemistry because of their several bioactivities such as antimicrobial [17, 18], antiamoebic [19], antinociceptive [20], anticancer [21], antidepressant [22] and anti-inflammatory [23].

Pyrazoline derivatives are typical intramolecular charge transfer (ICT) compounds owing to charge transfer from the nitrogen atom at the 1-position of pyrazoline to the carbon atom at the 3-position of the pyrazoline ring (Scheme 1). The effects of the solvents used on the absorbance and fluorescence properties of these ICT materials take attention to the researchers working in the fields [24-27]. The interactions between fluorescent probes and solvent molecules occur as either specifically (hydrogen bond etc.) or non-specifically. Multiple linear regression analysis suggested by Kamlet-Taft and Catalan is used to characterize the solvent–solute interactions. These approaches can be described by the following equations:

$$y = y_0 + a\alpha + b\beta + c\pi^* \quad \text{(Kamlet-Taft)} \qquad (1)$$

$$y = y_0 + aSA + bSB + cSP + dSdP \quad \text{(Catalan)} \qquad (2)$$

where y is the desired spectral property and y_0 stands spectral property in a vacuum or the gas phase. α, β and π* denote the hydrogen bond donor (HBD) acidity, hydrogen bond acceptor (HBA) basicity and dipolarity/polarizability of the solvents respectively. Catalan model parameters SA, SB, SP and SdP characterize the solvent acidity, basicity, polarizability and dipolarity respectively. a–d are the regression coefficients describing the sensitivity of the respective property to the different types of solvent–solute interactions [28-31].

In this study, it was aimed to investigate the spectral behaviors of the novel synthesized pyrazoline derivatives (4-[3-(4-Hydroxyphenyl)-5-aryl-4,5-dihydro-pyrazol-1-yl]benzenesulfonamides, **1-7,** Scheme 1) in different solvents. The substituents on the 4-position of phenyl ring were changed as hydrogen (1), methyl (2), methoxy (3), bromine (4), chlorine (5), flour (6), nitro (7). For this purpose, to take UV-Vis absorption, steady-state and time-resolved fluorescence measurements for all compounds in different solvents were planned. Since the changes in the optical properties of pyrazolines may find application in several areas such as chemical, biological and multimolecular systems as previously mentioned above. It was also considered to explain the interactions between the solvents used and solute, i.e. the compound by using multiple linear regression analysis. Additionally, the influences of the solvents used on the photo-physical parameters such as the fluorescence quantum yield, fluorescence lifetime, radiative (k_r) and non-radiative (k_{nr}) rate constants and the effects of the substituents available at the 4-position of phenyl (Scheme 1) on the photo-physical behavior were considered to investigate.

2. Experimental

2.1. Material

All the solvents (Sigma and Merck), quinine sulfate (Fluka) and H_2SO_4 (Sigma) were purchased and used without further purification. The physical properties, polarity parameters, Kamlet-Taft and Catalan parameters of all solvents used in the study are listed in Table 1 and 2 [32, 33]. The stock solution of all compounds was prepared in ethanol. A certain amount of fresh probe samples in different solution was obtained from this stock solution by evaporating the solvent. For all measurements, the concentrations of compounds were 2.0×10^{-6} M. All the experiments were performed at room temperature.

2.2. Equipment

The UV-Vis absorption and fluorescence spectra of the samples were recorded with Perkin Elmer Lambda 35 UV/VIS spectrophotometer and Shimadzu RF-5301PC spectrofluorophotometer, respectively. Fluorescence and absorption measurements were taken for all sulfonamide derivatives at room temperature. For the steady-state fluorescence measurements, all the samples were excited at 350 nm and fluorescence intensity were recorded between 355 nm and 650 nm. The fluorescence lifetime measurements were carried out with a LaserStrobe model TM3 spectrofluorophotometer from Photon Technology International (PTI). The excitation source combined a pulsed nitrogen laser/tunable dye laser. The samples were excited at 366 nm. The decay curves were collected over 200 channels using a nonlinear time scale with the time increment increasing according to arithmetic progression. The fluorescence decays were analyzed with the lifetime distribution analysis software from the instrument supplying company. The quality of fits was assessed by χ^2 values and weighed residuals [34]. The Fluorescence quantum yields of donor molecules were calculated through the Parker-Rees equation:

$$\emptyset_s = \emptyset_r \left(\frac{D_S}{D_r}\right)\left(\frac{\eta_s^2}{\eta_r^2}\right)\left(\frac{1-10^{-OD_r}}{1-10^{-OD_s}}\right) \quad (3)$$

where D is the integrated area under the corrected fluorescence spectrum, n is the refractive index of the solution, and O_D is the optical density at the excitation wavelength (λ_{ex}= 350 nm).

The subscripts *s* and *r* refer to the sample and reference solutions, respectively. Quinine sulfate in 0.5 M H_2SO_4 solution was used as the reference. The fluorescence quantum yield of quinine sulfate was 0.55 in 0.5 M H_2SO_4 solution [35].

The rate constants of the radiative (k_r) and non-radiative (k_{nr}) deactivation were calculated by using the following equations.

$$k_r = \frac{\Phi}{\tau_{av}} \quad (4)$$

$$\frac{1}{\tau_{av}} = k_r + k_{nr} \quad (5)$$

where Φ is fluorescence quantum yield and τ_{av} is average fluorescence lifetime of samples [36].

2.3.Synthesis of pyrazoline derivatives

The compounds were synthesized and characterized as described in our previous study [37]. The synthesis of the compounds has been summarized in Scheme 2. ^{1}H NMR, ^{13}C NMR, HRMS data, yield of the reactions and melting points of the compounds for compound **1-7** can be found in the supplementary file.

3. Results and discussion

3.1. Effect of solvents on absorption and fluorescence spectra

The absorption and fluorescence spectra of seven pyrazoline derivatives (Scheme 1) were recorded in ten different solvents such as 1,4-dioxane, tetrahydrofuran (THF), ethyl acetate, dimethyl formamide (DMF), dimethyl sulfoxide (DMSO), acetonitrile (ACN), isopropanol (i-PrOH), ethanol (EtOH), methanol (MeOH), water at room temperature (Figs. 1-2). Maximum absorption band for the compound **1** used were at about 350-360 nm (Fig. 1). The bands at issue were attributed to the $\pi \rightarrow \pi^*$ transitions of conjugated skeleton localized on the pyrazoline ring. The changes in the absorption maxima of the compounds depending on solvent polarity were presented in Table 3. The absorption maxima for each molecule shifted to longer wavelength

(bathochromic shift) and the intensity of absorbance decreased (hypochromic shift) when the solvent polarity increased. The bathochromic shifts are result from the increase in the dipole moment of the probe whereas the hypochromic shifts are result from the hydrogen-bond formation [38, 39]. It was observed that the shifts in absorption maxima were minimal comparing to maxima of fluorescence spectra of the compounds depending on solvent polarity. This suggested that there was no charge transfer in the ground state of the compounds.

The steady-state fluorescence and normalized fluorescence spectra of compound **1** were shown in Figs. 2 and 3. As shown in Fig. 2, the compound studied exhibited one broad band which represented $S_1 \rightarrow S_0$ electronic transition. It was observed that the red shifts in the fluorescence maxima with the increase in solvent polarity were greater than red shifts in the absorption maxima (Figs. S1 and S2). The energies of excited state of compounds were more affected from the increases in the solvent polarity comparing to the energies of the ground state of the compounds since there were differences between the shifts of fluorescence maxima and the shifts of absorption maxima in red region (Table 3) [26, 40]. The red shift observed depending on the solvent polarity indicated the presence of $\pi \rightarrow \pi^*$ transition. The shifts of fluorescence band maxima to the longer wavelength proved the presence of significant differences between excited and ground state charge distributions of the molecules. The reason of differences in charge distributions of the molecules was stronger intermolecular interactions in polar solvents in the excited state of the compounds [41]. The molar absorption coefficient (ε) values of the studied compounds were presented in Table 3. These values were remarkably high suggesting that the electronic transitions in the solvents from the ground state to the excited state had $\pi \rightarrow \pi^*$ character [10, 39].

The fluorescence quantum yield and lifetime values of fluorophores also changed depending on solvent polarity because the emission spectra influenced from solvent polarity. The values in question for the compounds in different solvents were listed in Table 3. The data obtained

revealed that significantly dependent to the solvent properties such as hydrogen bond donor ability, hydrogen bond acceptor ability and polarizability. The fluorescence quantum yields increased when solvent polarity increased in both polar aprotic (except for acetonitrile) and polar protic solvents. On the other hand, the fluorescence quantum yields had lower values in strongly polar solvent such as acetonitrile and alcohols comparing to the other solvents having less polarity. This phenomenon can be explained by positive solvatokinetic effects. In strong polar solvents, strong interactions between molecule and solvents occur when solvent polarity increased in excited state. When hydrogen bond interaction between a molecule and a proton donor solvent took place, the quantum yield of the compound decrease. The decreases in the quantum yield result from the fluorescence quenching whose reasons are the enhancement of intersystem crossing, strong internal conversion and vibrational deactivation all the reasons mentioned led to intramolecular charge transfer (ICT). This situation caused to increases in the rate of non-radiative relaxation of an excited state. This suggested that the positive solvatokinetic effect was taking place [10, 42].

To understand the dependence of the absorption and fluorescence spectra to the solvent, the solvent polarity parameter ($E_T(30)$) approach has been used. The Stokes shift ($\Delta\nu = \nu_{abs} - \nu_{flu}$) versus $E_T(30)$ were plotted (Fig. 4). A linear variation was obtained between the Stokes shift and the $E_T(30)$ values for the compounds studied. The linear variations implied potential application of these parameters to explain the microenvironment of the compounds which are new pyrazoline derivatives [43, 44].

Lippert–Mataga equation can be used to determine the influence of solvent polarity on the optical properties of a fluorophore [45-48]:

$$\Delta\nu = \nu_{abs} - \nu_{flu} = \frac{2\Delta\mu^2}{hca^3}\Delta f + constant \qquad (6)$$

where $\Delta\nu$ is the Stokes shift in wavenumber (cm^{-1}), ν_{abs} and ν_{flu} are the wavenumbers of the absorption and fluorescence maximum wavelengths, respectively, h is the Planck constant, c is

the light velocity, a is the cavity radius, and Δf is the orientation polarizability of the solvent defined as follows (Eq. 7):

$$\Delta f = \frac{\varepsilon-1}{2\varepsilon+1} - \frac{\eta^2-1}{2\eta^2+1} \quad (7)$$

where ε and η are the dielectric constant and refractive index of the solvent, respectively. Fig. 5 showed the plot of Stokes shift versus the orientation polarizability (Δf). The polar protic solvents were not included when the Fig. 5 was drawing due to specific solute–solvent interactions such as hydrogen bonding and the acidity and basicity of solvents. The linear relationships between Stokes shift versus the orientation polarizability indicated that the Stokes shift was dependent to the solvent dipolarity and/or polarizability. For all compounds, the differences in between dipole moments (Δμ) of the ground and excited states were calculated from the Lippert–Mataga equation. At this equation, the cavity radius a for all compounds was estimated by using Eq. (8)

$$a = \left(\frac{3M}{4N\pi d}\right)^{1/3} \quad (8)$$

where M is the molecular weight, N is Avogadro's number, and d is an assumed molecular density of 1 g cm^{-3}. The estimated dipole moment differences were 19.93, 27.18, 28.90, 15.77, 17.21, 18.36 and 27.81 of compounds **1-7,** respectively. These large dipole moment differences indicated that the intramolecular charge transfer (ICT) state occurred by the effect of the solvent used after the excitation of the compounds [38].

3.2. Multiple regression analysis

Multiple linear regression analysis suggested by Kamlet-Taft (Eq.1) and Catalan (Eq.2) were also employed to discuss the solvent effects in more detail. The regression coefficients, their standard deviations and the multiple linear correlation coefficient r for the pyrazoline derivatives were summarized in Tables 4 and 5. It was noticed that the largest contribution to the interactions between a solute and a solvent belonged to the solvent dipolarity/polarizability ($c\pi^*$ and cSP). This indicated that the dominant factor on the solvatochromic changes in

absorption wavelength (λ_{abs}) and fluorescence wavelength (λ_{flu}) was the solvent polarizability. However, the contributions of hydrogen bond donor (HBD) acidity and hydrogen bond acceptor (HBA) parameters in solvent cannot be neglected. The multiple regression analysis of ν_{abs} and ν_{flu} indicated that HBD/solvent acidity (α/SA) much more contributed to interaction between a solute and a solvent than HBA/solvent basicity (β/SB) for all compounds tested. The low values of α and β compared to π^* supported that spectroscopic properties of these pyrazoline derivatives were less sensitive to hydrogen bonding characteristics of solvents. These results were supported by those obtained from the $E_T(30)$ approach and the Lippert–Mataga approach [41, 49]. Negative values of regression coefficients indicated that the regression parameters considered contributed to the stabilization of the compounds both the ground state and the excited state [50].

3.3. Substituent effect

Seven novel pyrazoline derivatives synthesized and studied here had different at the substituents groups 4- position of phenyl ring (Scheme 1). The compounds **1-6** exhibited very high fluorescence properties in the blue-green region. The intensity in fluorescence spectra of each compound in DMSO changed depending on the nature of substituents on phenyl rings (Fig. 6). Increases in fluorescence intensity of the substituted compounds (**2-6**) were observed comparing to compound **1** which is non-substituted derivative without dependent the electronic nature of the substituent on phenyl ring (i.e. electron donating and electron withdrawing substituent), exception was the compound **7** which has nitro substituent on phenyl ring. In the case of the compound **7**, the efficient intersystem crossing process occur due to the existence of a low-lying $n \rightarrow \pi^*$ transition. The presence of detectable fluorescence decrease results from high rate of $S_1 \rightarrow S_0$ internal conversion. $S_1 \rightarrow S_0$ internal conversion may be related to the considerable charge transfer character of the excited state of nitro bearing compound, since $-NO_2$ group has strong electron-withdrawing nature [51]. The fluorescence quantum yield

values of the compounds **2-6** were higher than the compound 1's, which is non-substituted compound, without dependent the nature of substituents (i.e. electron donating and electron withdrawing substituent) except the compound **7**. This situation was similar to the situation fluorescence intensity as mentioned before.

The values as the fluorescence intensities and quantum yields obtained in this study were remarkably higher than the ones reported in literatures for the compounds having pyrazoline moiety [10, 39, 52-56]. The data obtained from the present study may be useful in pharmaceutical industry, in labeling and sensor applications as biosensors or analytical sensors.

4. Conclusions

The photo-physical behaviors of newly synthesized seven pyrazoline derivatives **1-7** (Scheme 1) were described in different solvents. All compounds (except for **7**) exhibited very high fluorescence properties depending on the solvent polarity in the blue-green region. It was observed that the energy of excited state for every compound was more affected from the increases in the solvent polarity compared to the energy of ground state of the same compound. This situation suggested the presence of significant differences between excited and ground state charge distributions of the molecules. The solvent dependence of the absorption and fluorescence spectra was discussed using the solvent polarity parameter ($E_T(30)$) approach, Lippert–Mataga equation, and multiple linear regression analysis. All results shown in Fig. 4, Fig. 5 and Table 4, Table 5 pointed out that the dominant factor affecting the interaction between a solute (compound) and a solvent was the solvent polarizability on the solvatochromic changes in λ_{abs} and λ_{flu}. In addition, the fluorescence quantum yield values calculated for compounds **1-7** comparing to the previous values of several compounds having pyrazoline ring in literatures in different solvents were quite impressive and high. Moreover, the effects of the substituent at 4-position of phenyl ring on the photo-physical properties of the compounds **1-7** were evaluated. The increases in fluorescence intensities and the fluorescence quantum yields were noticed in compounds **2-6** without dependent to the electronic nature of the substituents

comparing to non-substituent compound, except compound **7** which has nitro group. The photo-physical properties of these biologically active novel molecular probes may be useful in some areas, such as labeling, sensor applications in different environments.

REFERENCES

[1] T. Peng, X. Chen, L. Gao, T. Zhang, W. Wang, J. Shen, D. Yang, A rationally designed rhodamine-based fluorescent probe for molecular imaging of peroxynitrite in live cells and tissues, Chemical Science, (2016).
[2] A.V. Saura, M.J. Marin, M.I. Burguete, D.A. Russell, F. Galindo, S.V. Luis, The synthesis of new fluorescent bichromophoric compounds as ratiometric pH probes for intracellular measurements, Organic & Biomolecular Chemistry, 13 (2015) 7736-7749.
[3] B.R. Raju, M.M.T. Carvalho, M.I.P.S. Leitão, P.J.G. Coutinho, M.S.T. Gonçalves, Synthesis, photophysical characterisation and photostability studies of NIR probes with aliphatic, aromatic and chlorinated terminals in 5- and 9-amino positions of benzo[a]phenoxazines, Dyes and Pigments, 132 (2016) 204-212.
[4] J.L. Westrup, L.W. Oenning, M.M. da Silva Paula, R. da Costa Duarte, F.S. Rodembusch, T.E.A. Frizon, L. da Silva, A.G. Dal-Bó, New photoactive D-π-A-π-D benzothiadiazole derivative: Synthesis, thermal and photophysical properties, Dyes and Pigments, 126 (2016) 209-217.
[5] D.-H. Lee, D.-N. Lee, J.-I. Hong, A fluorescent probe for a lewisite simulant, New Journal of Chemistry, (2016).
[6] H. Agnihotri, M. Paramasivam, V. Palakollu, S. Kanvah, Photoisomerization of Trans Ortho-, Meta-, Para-Nitro Diarylbutadienes: A Case of Regioselectivity, Photochemistry and Photobiology, 91 (2015) 1324-1331.
[7] J.C. del Valle, C. Díaz-Oliva, Steady-State Spectroscopy of the 2-(N-methylacetimidoyl)-1-naphthol Molecule, Photochemistry and Photobiology, 91 (2015) 660-671.
[8] Y. Niko, Y. Cho, S. Kawauchi, G.-i. Konishi, Pyrene-based D-[small pi]-A dyes that exhibit solvatochromism and high fluorescence brightness in apolar solvents and water, RSC Advances, 4 (2014) 36480-36484.
[9] B. Varghese, S.H. Al-Harthi, S.N. Al-Busafi, F.O. Suliman, S.M.Z. Al-Kindy, M.T. Zar Myint, Influence of anchoring of a pyrazoline dye 3-naphthyl-1-phenyl-5 (4-amino phenyl)-2-pyrazoline (NPAP) in manipulating the electronic and chemical properties of a graphene oxide via amidation: Synthesis, characterization and photophysics, Journal of Luminescence, 192 (2017) 527-533.
[10] B. Varghese, S.N. Al-Busafi, F.O. Suliman, S.M.Z. Al-Kindy, Synthesis, spectroscopic characterization and photophysics of a novel environmentally sensitive dye 3-naphthyl-1-phenyl-5-(4-carboxyphenyl)-2-pyrazoline, Journal of Luminescence, 159 (2015) 9-16.
[11] X.H. Zhang, S.K. Wu, Z.Q. Gao, C.S. Lee, S.T. Lee, H.L. Kwong, Pyrazoline derivatives for blue color emitter in organic electroluminescent devices, Thin Solid Films, 371 (2000) 40-46.
[12] P. Stakhira, S. Khomyak, V. Cherpak, D. Volyniuk, J. Simokaitiene, A. Tomkeviciene, N.A. Kukhta, J.V. Grazulevicius, A.V. Kukhta, X.W. Sun, H.V. Demir, Z. Hotra, L. Voznyak, Blue organic light-emitting diodes based on pyrazoline phenyl derivative, Synthetic Metals, 162 (2012) 352-355.
[13] M.M. Ibrahim, M. Al-Refai, K. Ayub, B.F. Ali, Synthesis, Spectral Characterization and Fluorescent Assessment of 1,3,5-Triaryl-2-pyrazoline Derivatives: Experimental and Theoretical Studies, Journal of Fluorescence, (2016) 1-9.

[14] V. Ramkumar, P. Kannan, Novel heterocyclic based blue and green emissive materials for opto-electronics, Optical Materials, 46 (2015) 314-323.
[15] S. Urinda, G. Das, A. Pramanik, P. Sarkar, Theoretical studies on the photophysical properties of some Iridium (III) complexes used for OLED, Journal of Physics and Chemistry of Solids, 96 (2016) 100-106.
[16] S. Urinda, G. Das, A. Pramanik, P. Sarkar, Tuning the phosphorescence and quantum efficiency of heteroleptic Ir(III) complexes based on pyridine-tetrazole as an ancillary ligand: An overview from quantum chemical investigations, Computational and Theoretical Chemistry, 1092 (2016) 32-40.
[17] A. Ahmad, A. Husain, S.A. Khan, M. Mujeeb, A. Bhandari, Synthesis, antimicrobial and antitubercular activities of some novel pyrazoline derivatives, Journal of Saudi Chemical Society.
[18] A. Sid, A. Messai, C. Parlak, N. Kazancı, D. Luneau, G. Keşan, L. Rhyman, I.A. Alswaidan, P. Ramasami, 1-Formyl-3-phenyl-5-(4-isopropylphenyl)-2-pyrazoline: Synthesis, characterization, antimicrobial activity and DFT studies, Journal of Molecular Structure, 1121 (2016) 46-53.
[19] H. Parveen, S. Mukhtar, A. Azam, Novel Ferrocenyl Linked Pyrazoline Analogs as Potent Antiamoebic Agents, Journal of Heterocyclic Chemistry, 53 (2016) 473-478.
[20] I.F. Florentino, P.M. Galdino, L.P. De Oliveira, D.P.B. Silva, F. Pazini, F.A. Vanderlinde, L.M. Lião, R. Menegatti, E.A. Costa, Involvement of the NO/cGMP/KATP pathway in the antinociceptive effect of the new pyrazole 5-(1-(3-fluorophenyl)-1H-pyrazol-4-yl)-2H-tetrazole (LQFM-021), Nitric Oxide, 47 (2015) 17-24.
[21] M. Karabacak, M. Altıntop, H. İbrahim Çiftçi, R. Koga, M. Otsuka, M. Fujita, A. Özdemir, Synthesis and Evaluation of New Pyrazoline Derivatives as Potential Anticancer Agents, Molecules, 20 (2015) 19066.
[22] A. Özdemir, M. Altıntop, Z. Kaplancıklı, Ö. Can, Ü. Demir Özkay, G. Turan-Zitouni, Synthesis and Evaluation of New 1,5-Diaryl-3-[4-(methyl-sulfonyl)phenyl]-4,5-dihydro-1H-pyrazole Derivatives as Potential Antidepressant Agents, Molecules, 20 (2015) 2668.
[23] M.A. Abdel-Sayed, S.M. Bayomi, M.A. El-Sherbeny, N.I. Abdel-Aziz, K.E.H. ElTahir, G.S.G. Shehatou, A.A.M. Abdel-Aziz, Synthesis, anti-inflammatory, analgesic, COX-1/2 inhibition activities and molecular docking study of pyrazoline derivatives, Bioorganic & Medicinal Chemistry, 24 (2016) 2032-2042.
[24] Y. Zhang, M. Jiang, G.-C. Han, K. Zhao, B.Z. Tang, K.S. Wong, Solvent Effect and Two-Photon Optical Properties of Triphenylamine-Based Donor–Acceptor Fluorophores, The Journal of Physical Chemistry C, 119 (2015) 27630-27638.
[25] Y. Li, M. Zhou, Y. Niu, Q. Guo, A. Xia, Solvent-dependent intramolecular charge transfer delocalization/localization in multibranched push-pull chromophores, The Journal of Chemical Physics, 143 (2015) 034309.
[26] R. Alphonse, A. Varghese, L. George, A. Nizam, Estimation of ground state and excited state dipole moments of a novel Schiff base derivative containing 1, 2, 4-triazole nucleus by solvatochromic method, Journal of Molecular Liquids, 215 (2016) 387-395.
[27] T.V. Y, D.S. Agarwal, A. Sarmah, L. Joshi, R. Sakhuja, D.D. Pant, Solvent effects on the absorption and emission spectra of novel (E)-4-((4-(heptyloxy)phenyl)diazenyl)benzyl (((9H-fluoren-9-yl)methoxy)carbonyl)-d-alaninate (Fmoc-al-az): Determination of dipole moment by experimental and theoretical study, Journal of Molecular Structure, 1129 (2017) 248-255.
[28] H.S. Geethanjali, R.M. Melavanki, D. Nagaraja, N.R. Patil, J. Thipperudrappa, R.A. Kusanur, Specific interactions of alcohols and non-alcohols with a biologically active boronic acid derivative: a spectroscopic study, Luminescence, 31 (2016) 1046-1053.
[29] A. Alimmari, B. Božić, D. Mijin, A. Marinković, N. Valentić, G. Ušćumlić, Synthesis, structure and solvatochromic properties of some novel 5-arylazo-6-hydroxy-4-(4-

methoxyphenyl)-3-cyano-2-pyridone dyes: Hydrazone-azo tautomeric analysis, Arabian Journal of Chemistry, 8 (2015) 269-278.
[30] M. Khadem Sadigh, M.S. Zakerhamidi, S.M. Seyed Ahmadian, M. Johari-Ahar, L. Zare Haghighi, Environment and solute-solvent interaction effects on photo-physical behaviors of Folic acid and Folinic acid drugs, Journal of Molecular Structure, 1125 (2016) 177-185.
[31] B. Maity, A. Chatterjee, D. Seth, Photophysics of a Coumarin in Different Solvents: Use of Different Solvatochromic Models, Photochemistry and Photobiology, 90 (2014) 734-746.
[32] J. Catalán, Toward a Generalized Treatment of the Solvent Effect Based on Four Empirical Scales: Dipolarity (SdP, a New Scale), Polarizability (SP), Acidity (SA), and Basicity (SB) of the Medium, The Journal of Physical Chemistry B, 113 (2009) 5951-5960.
[33] C. Reichardt, Solvatochromic Dyes as Solvent Polarity Indicators, Chemical Reviews, 94 (1994) 2319-2358.
[34] E. Bozkurt, M. Arık, Y. Onganer, A novel system for Fe3+ ion detection based on fluorescence resonance energy transfer, Sensors and Actuators B: Chemical, 221 (2015) 136-147.
[35] A.M. Brouwer, Standards for photoluminescence quantum yield measurements in solution (IUPAC technical report), Pure and Applied Chemistry, 83 (2011) 2213-2228.
[36] A. Jana, B. Das, S.K. Mandal, S. Mabhai, A.R. Khuda-Bukhsh, S. Dey, Deciphering the CHEF-PET-ESIPT liaison mechanism in a Zn2+ chemosensor and its applications in cell imaging study, New Journal of Chemistry, 40 (2016) 5976-5984.
[37] H.I. Gul, E. Mete, S.E. Eren, H. Sakagami, C. Yamali, C.T. Supuran, Designing, synthesis and bioactivities of 4-[3-(4-hydroxyphenyl)-5-aryl-4,5-dihydro-pyrazol-1-yl]benzenesulfonamides, Journal of Enzyme Inhibition and Medicinal Chemistry, (2016) 1-7.
[38] S. Song, D. Ju, J. Li, D. Li, Y. Wei, C. Dong, P. Lin, S. Shuang, Synthesis and spectral characteristics of two novel intramolecular charge transfer fluorescent dyes, Talanta, 77 (2009) 1707-1714.
[39] B. Varghese, S.N. Al-Busafi, F.O. Suliman, S.M.Z. Al-Kindy, Study on the spectral and inclusion properties of a sensitive dye, 3-naphthyl-1-phenyl-5-(5-fluoro-2-nitrophenyl)-2-pyrazoline, in solvents and β-cyclodextrin, Spectrochimica Acta Part A: Molecular and Biomolecular Spectroscopy, 136, Part B (2015) 661-671.
[40] N.R. Patil, R.M. Melavanki, S.B. Kapatkar, N.H. Ayachit, J. Saravanan, Solvent Effect on Absorption and Fluorescence Spectra of Three Biologically Active Carboxamides (C1, C2 and C3). Estimation of Ground and Excited State Dipole Moment from Solvatochromic Method Using Solvent Polarity Parameters, Journal of Fluorescence, 21 (2011) 1213-1222.
[41] U.P. Raghavendra, M. Basanagouda, R.M. Melavanki, R.H. Fattepur, J. Thipperudrappa, Solvatochromic studies of biologically active iodinated 4-aryloxymethyl coumarins and estimation of dipole moments, Journal of Molecular Liquids, 202 (2015) 9-16.
[42] Z. Zhang, P. Xue, P. Gong, G. Zhang, J. Peng, R. Lu, Mechanofluorochromic behaviors of [small beta]-iminoenolate boron complexes functionalized with carbazole, Journal of Materials Chemistry C, 2 (2014) 9543-9551.
[43] S.A. El-Daly, A.M. Asiri, K. Alamry, S.A. Khan, Spectroscopic studies and laser activity of 3-(4-dimethylamino-phenyl)-1-(2,5-dimethyl-furan-3-yl)-propenone (DDFP): A new green laser dye, Journal of Luminescence, 137 (2013) 6-14.
[44] S.M. Afzal, A.M. Asiri, M.A.N. Razvi, A.H. Bakry, S.A. Khan, M.E.M. Zayed, Synthesis, Spectrofluorometric Studies, Micellization and non Linear Optical Properties of Blue Emitting Quinoline (AMQC) Dye, Journal of Fluorescence, 26 (2016) 559-566.
[45] H. Liu, X. Xu, H. Peng, X. Chang, X. Fu, Q. Li, S. Yin, G.J. Blanchard, Y. Fang, New solvatochromic probes: performance enhancement via regulation of excited state structures, Physical Chemistry Chemical Physics, 18 (2016) 25210-25220.

[46] M. Fujii, M. Namba, M. Yamaji, H. Okamoto, Solvent-induced multicolour fluorescence of amino-substituted 2,3-naphthalimides studied by fluorescence and transient absorption measurements, Photochemical & Photobiological Sciences, 15 (2016) 842-850.
[47] D. Prukala, I. Khmelinskii, J. Koput, M. Gierszewski, T. Pędziński, M. Sikorski, Photophysics, Excited-state Double-Proton Transfer and Hydrogen-bonding Properties of 5-Deazaalloxazines, Photochemistry and Photobiology, 90 (2014) 972-988.
[48] A.A. Abdel-Shafi, M.A. Ismail, S.S. Al-Shihry, Effect of solvent and encapsulation in β-cyclodextrin on the photophysical properties of 4-[5-(thiophen-2-yl)furan-2-yl]benzamidine, Journal of Photochemistry and Photobiology A: Chemistry, 316 (2016) 52-61.
[49] T. Nakahama, D. Kitagawa, H. Sotome, S. Ito, H. Miyasaka, S. Kobatake, Optical properties and solvatofluorochromism of fluorene derivatives bearing S,S-dioxidized thiophene, Photochemical & Photobiological Sciences, (2016).
[50] A. Mishra, G. Krishnamoorthy, Photophysical study of 2-(4[prime or minute]-N,N-dimethylaminophenyl)oxazolo[4,5-b]pyridine in different solvents and at various pH, Photochemical & Photobiological Sciences, 11 (2012) 1356-1367.
[51] B. Valeur, M.N. Berberan-Santos, Molecular fluorescence: principles and applications, John Wiley & Sons, 2012.
[52] A. Sarkar, T. Kumar Mandal, D. Kumar Rana, S. Dhar, S. Chall, S. Chandra Bhattacharya, Tuning the photophysics of a bio-active molecular probe '3-pyrazolyl-2-pyrazoline' derivative in different solvents: Dual effect of polarity and hydrogen bonding, Journal of Luminescence, 130 (2010) 2271-2276.
[53] S.-Q. Wang, Y. Gao, H.-Y. Wang, X.-X. Zheng, S.-L. Shen, Y.-R. Zhang, B.-X. Zhao, Synthesis, X-ray crystal structure and optical properties of novel 1,3,5-triarylpyrazoline derivatives and the fluorescent sensor for Cu2+, Spectrochimica Acta Part A: Molecular and Biomolecular Spectroscopy, 106 (2013) 110-117.
[54] J. Ajantha, E. Varathan, V. Bharti, V. Subramanian, S. Easwaramoorthi, S. Chand, Photophysical and charge transport properties of pyrazolines, RSC Advances, 6 (2016) 786-795.
[55] B. Dong, M. Wang, C. Xu, Synthesis, photoluminescence properties and theoretical insights on 1,3-diphenyl-5-(9-anthryl)-2-pyrazoline and -1H-pyrazole, Luminescence, 28 (2013) 628-633.
[56] V. Ramkumar, P. Kannan, Thiophene and furan containing pyrazoline luminescent materials for optoelectronics, Journal of Luminescence, 169, Part A (2016) 204-215.

Figr-1**FIGURES CAPTION**

Scheme 1. Structure of the pyrazoline derivatives **1-7**

Scheme 2. Synthesis of the pyrazoline derivatives **1-7**

Fig. 1. The absorption spectra of compound **1** in different solvents.

Fig. 2. The fluorescence spectra of compound **1** in different solvents.

Fig. 3. Normalized fluorescence spectra of compound **1** in different solvents.

Fig. 4. The plot of Stokes shift versus the solvent polarity, $E_T(30)$

Fig. 5. Stokes shift ($\Delta\nu = \nu_{abs} - \nu_{flu}$ /cm^{-1}) versus orientation polarizability function (Δf).

Fig. 6. The fluorescence spectra of pyrazoline derivatives, **1-7** in DMSO.

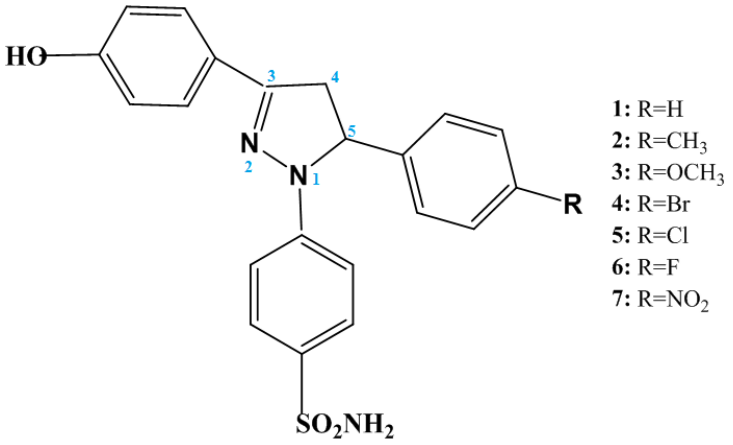

Scheme 1.

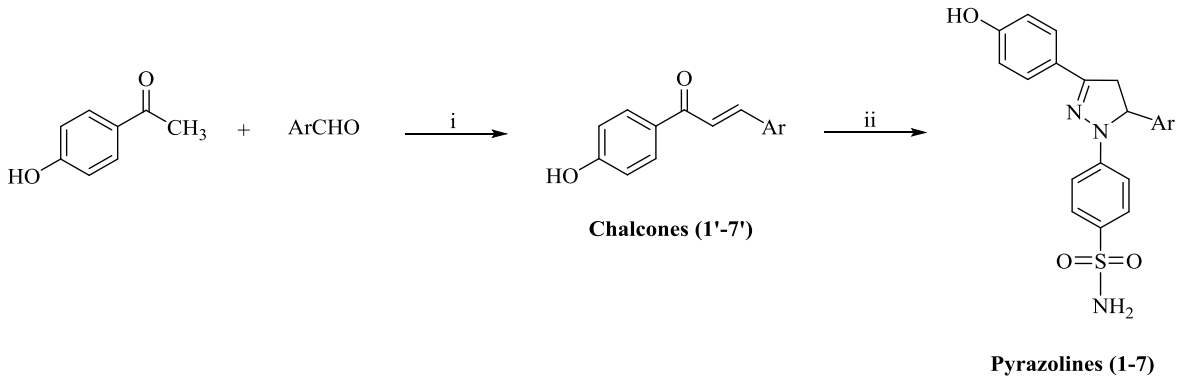

Reagents and conditions. (i) 10% aq NaOH, EtOH, 0-5 ºC, 12 h; (ii) 4-Hydrazinobenzenesulfonamide hydrochloride, EtOH, glacial acetic acid, reflux 6-12 h. **Ar:** C_6H_5 for **1′, 1;** 4-$CH_3C_6H_4$ for **2′, 2;** 4-$CH_3OC_6H_4$ for **3′, 3;** 4-BrC_6H_4 for **4′, 4;** 4-ClC_6H_4 for **5′, 5;** 4-FC_6H_4 for **6′, 6;** 4-$NO_2C_6H_4$ for **7′, 7**.

Scheme 2.

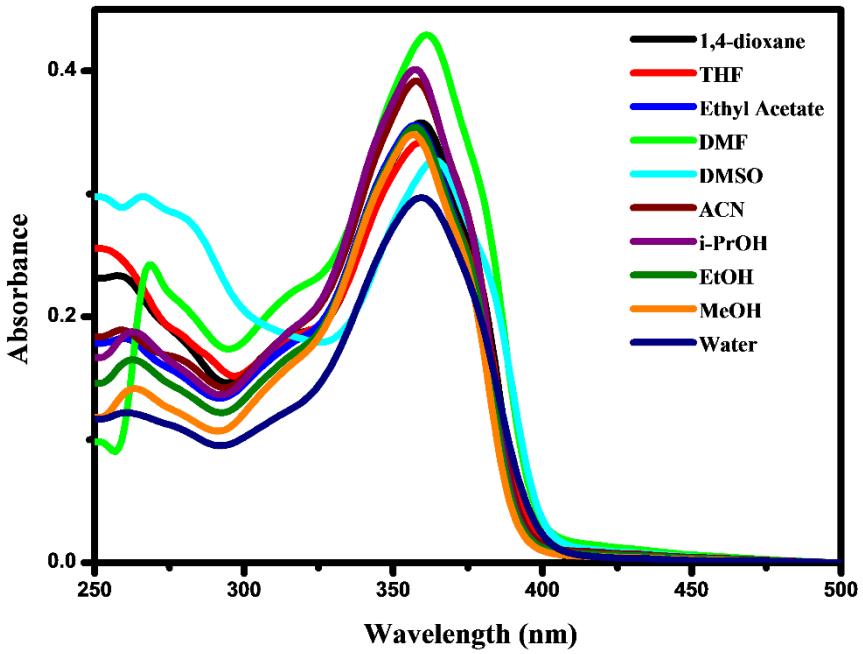

Fig. 1.

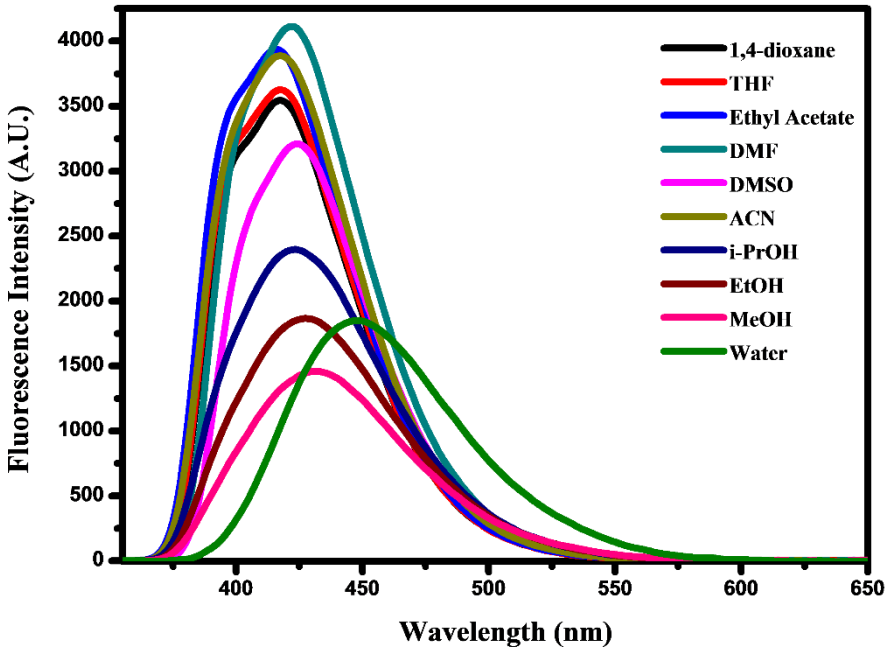

Fig. 2.

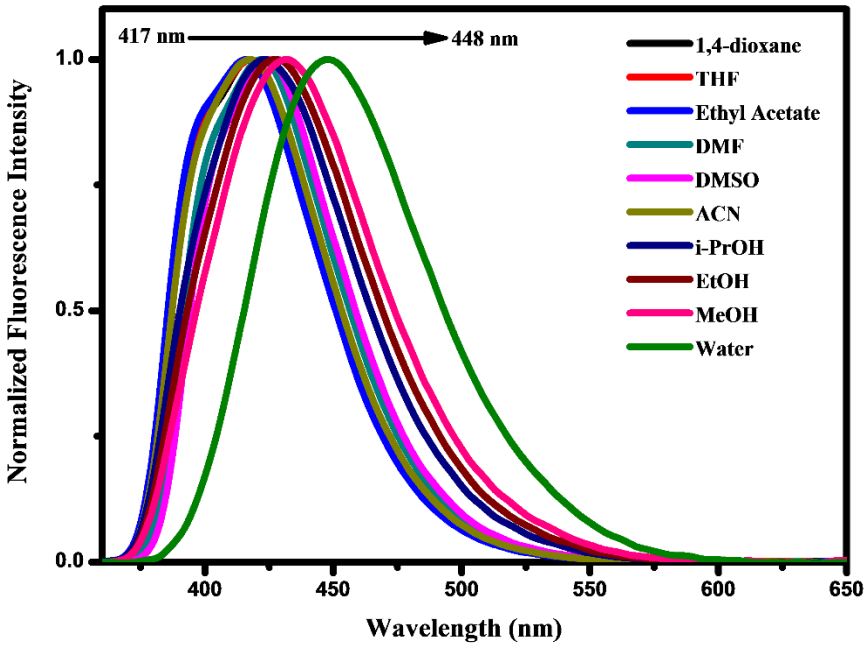

Fig. 3.

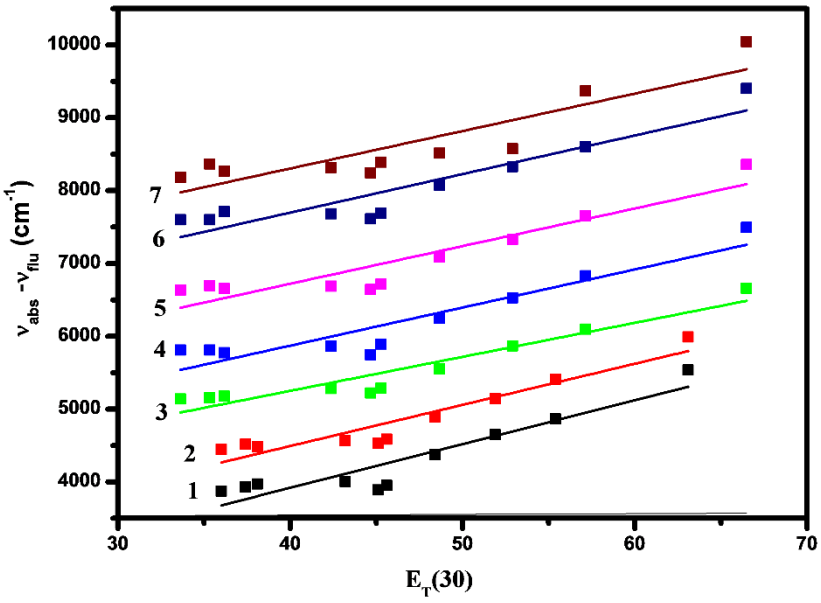

Fig. 4.

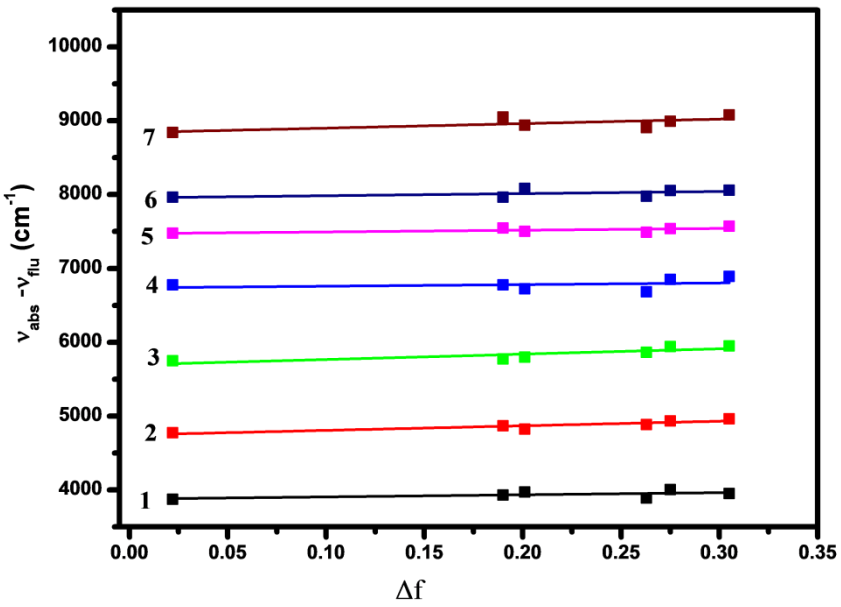

Fig. 5.

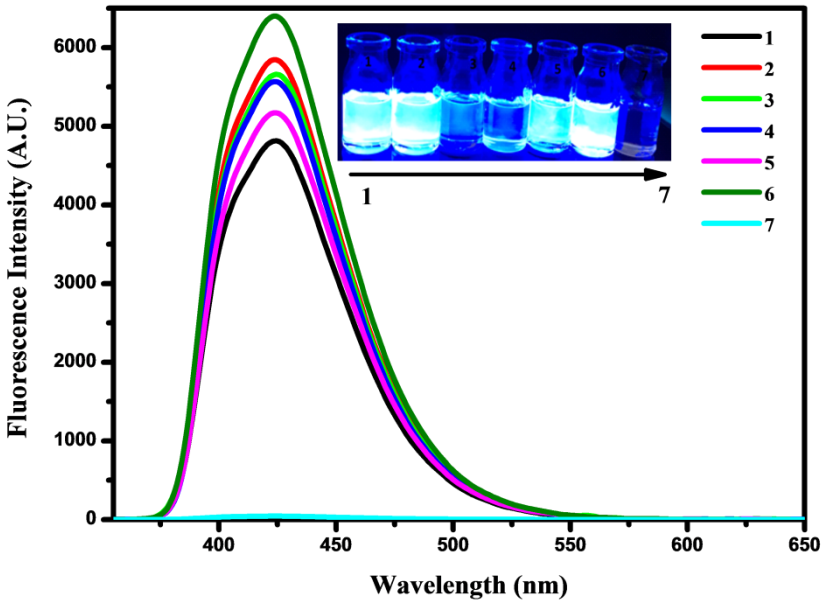

Fig. 6.

TABLES

Table 1. The physical properties and polarity parameters of selected solvents

Table 2. Kamlet-Taft and Catalan parameters of selected solvents

Table 3. Spectroscopic and photo-physical properties of compounds **1-7** in selected solvents

Table 4. Estimated coefficients (y_0, $a\alpha$, $b\beta$, $c\pi^*$ for ν_{abs}, ν_{flu}) and correlation coefficients (r) for regression analysis of the pyrazoline derivatives **1-7** according to the Kamlet-Taft solvent parameters

Table 5. Estimated coefficients (y_0, aSA, bSB, cSP and dSdP for ν_{abs}, ν_{flu}) and correlation coefficients (r) for regression analysis of the pyrazoline derivatives **1-7** according to the Catalan solvent parameters

Table 1.

Solvent	ε^a	η^b	$E_T(30)^c$	$E_T^{N(d)}$	f (ε,η)	g (η)
1,4-Dioxane	2.2	1.422	36.0	0.164	0.044	0.617
THF	7.5	1.465	37.4	0.207	0.521	1.151
Ethyl Acetate	6.1	1.372	38.1	0.228	0.493	0.999
DMF	36.7	1.430	43.2	0.386	0.836	1.419
DMSO	46.7	1.479	45.1	0.444	0.840	1.488
ACN	36.6	1.344	45.6	0.460	0.861	1.330
i-PrOH	20.2	1.377	48.4	0.546	0.781	1.294
EtOH	25.3	1.361	51.9	0.654	0.817	1.309
MeOH	33.0	1.329	55.4	0.762	0.855	1.304
Water	80.0	1.333	63.1	1.000	0.914	0.227

[a] Dielectric constant. [b] Refractive index. [c] Reichardt empirical polarity parameter. [d]Molecular-microscopic solvent polarity parameter. THF; tetrahydrofuran. DMF; dimethylformamide. DMSO; dimethyl sulfoxide. ACN; acetonitrile. i-PrOH; isopropanol. EtOH; ethanol. MeOH; methanol

Table 2.

Solvents	Kamlet-Taft Parameters			Catalan Parameters			
	α	β	π^*	SA	SB	SP	SdP
1,4-Dioxane	0.00	0.37	0.49	0.000	0.444	0.737	0.312
THF	0.00	0.55	0.55	0.000	0.591	0.714	0.634
Ethyl Acetate	0.00	0.45	0.45	0.000	0.542	0.656	0.603
DMF	0.00	0.69	0.88	0.031	0.613	0.759	0.977
DMSO	0.00	0.76	1.00	0.072	0.647	0.830	1.000
ACN	0.19	0.40	0.66	0.044	0.286	0.645	0.974
i-PrOH	0.76	0.84	0.48	0.283	0.830	0.633	0.808
EtOH	0.86	0.75	0.54	0.400	0.658	0.633	0.783
MeOH	0.98	0.66	0.60	0.605	0.545	0.608	0.904
Water	1.17	0.47	1.09	1.062	0.025	0.681	0.997

Table 3.

Compound	Solvent	λ_{abs} (nm)	ε (10^5 $M^{-1}cm^{-1}$)	λ_{em} (nm)	$\Delta\nu$ (cm^{-1})	Φ	τ_{av} (ns)	$k_r x10^{-9}$ (s^{-1})	$k_{nr} x10^{-9}$ (s^{-1})
1	1,4-Dioxane	359	3.58	417	3874	0.63	2.362	0.2665	0.1569
	THF	359	3.41	418	3932	0.65	2.313	0.2800	0.1523
	Ethyl Acetate	357	3.56	416	3973	0.66	2.267	0.2932	0.1479
	DMF	361	4.30	422	4004	0.68	2.400	0.2821	0.1346
	DMSO	364	3.27	424	3888	0.70	2.449	0.2840	0.1243
	ACN	358	3.92	417	3952	0.60	2.378	0.2519	0.1686
	i-PrOH	357	4.01	423	4371	0.44	1.859	0.2341	0.3038
	EtOH	357	3.54	428	4647	0.36	1.931	0.1864	0.3315
	MeOH	357	3.48	432	4863	0.28	1.619	0.1736	0.4441
	Water	359	2.97	448	5534	0.41	3.164	0.1310	0.1850
2	1,4-Dioxane	360	3.42	417	3797	0.73	2.411	0.3031	0.1117
	THF	359	4.17	417	3874	0.70	2.396	0.2907	0.1266
	Ethyl Acetate	358	4.30	415	3837	0.68	2.412	0.2801	0.1345
	DMF	362	3.99	422	3928	0.76	2.591	0.2924	0.0936
	DMSO	364	3.53	424	3888	0.82	2.557	0.3201	0.0710
	ACN	358	4.89	417	3952	0.64	2.316	0.2780	0.1538
	i-PrOH	358	4.59	423	4292	0.50	2.106	0.2351	0.2397
	EtOH	358	4.63	428	4568	0.43	2.037	0.2128	0.2781
	MeOH	357	4.73	432	4863	0.33	1.664	0.2010	0.4000
	Water	360	1.33	449	5506	0.55	3.348	0.1651	0.1336
3	1,4-Dioxane	360	3.80	418	3854	0.73	2.245	0.3250	0.1205
	THF	359	2.48	417	3874	0.78	2.358	0.3313	0.0928
	Ethyl Acetate	358	3.29	416	3894	0.76	2.333	0.3270	0.1017
	DMF	361	3.00	422	4004	0.87	2.504	0.3464	0.0530
	DMSO	364	3.32	425	3943	0.88	2.517	0.3486	0.0487
	ACN	358	4.40	418	4010	0.70	2.208	0.3158	0.1371
	i-PrOH	358	3.44	423	4292	0.55	1.997	0.2755	0.2252
	EtOH	358	4.22	429	4623	0.47	1.838	0.2553	0.2888
	MeOH	357	3.80	432	4863	0.38	1.676	0.2244	0.3723
	Water	360	1.22	448	5456	0.54	3.313	0.1624	0.1394
4	1,4-Dioxane	358	3.58	417	3952	0.75	2.174	0.3314	0.1132
	THF	358	3.68	417	3952	0.70	2.249	0.3230	0.1364
	Ethyl Acetate	357	3.95	415	3915	0.75	2.177	0.3435	0.1158
	DMF	361	4.03	422	4004	0.68	2.116	0.3208	0.1518
	DMSO	364	3.66	424	3888	0.69	2.004	0.3455	0.1535
	ACN	357	4.34	417	4030	0.65	2.197	0.2978	0.1574
	i-PrOH	357	3.84	423	4371	0.57	1.976	0.2870	0.2191
	EtOH	357	3.73	428	4647	0.50	1.840	0.2731	0.2703
	MeOH	356	4.40	432	4942	0.38	1.667	0.2296	0.3703
	Water	359	2.03	449	5583	0.56	3.073	0.1823	0.1431

Table 3. Continued

Compound	Solvent	λ_{abs} (nm)	ε (10^5 $M^{-1}cm^{-1}$)	λ_{em} (nm)	$\Delta\nu$ (cm^{-1})	Φ	τ_{av} (ns)	$k_r x10^{-9}$ (s^{-1})	$k_{nr} x10^{-9}$ (s^{-1})
5	1,4-Dioxane	358	2.90	417	3952	0.72	2.291	0.3103	0.1208
	THF	358	3.59	418	4010	0.68	2.320	0.2915	0.1358
	Ethyl Acetate	357	3.10	416	3973	0.72	2.340	0.3069	0.1205
	DMF	361	3.14	422	4004	0.71	2.355	0.3030	0.1217
	DMSO	363	3.61	424	3963	0.75	2.486	0.3008	0.1015
	ACN	357	3.09	417	4030	0.65	2.289	0.2851	0.1518
	i-PrOH	357	3.66	423	4371	0.53	1.998	0.2644	0.2361
	EtOH	357	4.58	427	4592	0.44	1.884	0.2315	0.2993
	MeOH	356	4.08	431	4888	0.36	1.679	0.2133	0.3823
	Water	359	1.34	448	5534	0.56	3.202	0.1752	0.1371
6	1,4-Dioxane	358	4.73	417	3952	0.78	2.329	0.3207	0.0925
	THF	358	3.59	417	3952	0.88	2.420	0.3748	0.0515
	Ethyl Acetate	356	2.75	416	4051	0.87	2.346	0.3688	0.0575
	DMF	360	4.03	421	4025	0.89	2.449	0.3618	0.0465
	DMSO	363	3.63	424	3963	0.93	2.451	0.3779	0.0301
	ACN	357	3.37	417	4030	0.75	2.243	0.3322	0.1136
	i-PrOH	357	4.79	423	4371	0.52	1.981	0.2631	0.2417
	EtOH	357	4.28	427	4592	0.47	1.780	0.2658	0.2960
	MeOH	356	3.92	430	4834	0.36	1.644	0.2201	0.3881
	Water	359	1.85	448	5534	0.57	3.171	0.1808	0.1345
7	1,4-Dioxane	353	2.92	417	4348	0.01	2.064	0.0032	0.4526
	THF	353	3.72	420	4519	0.01	2.194	0.0029	0.4183
	Ethyl Acetate	352	2.82	417	4428	0.01	2.374	0.0030	0.4182
	DMF	355	2.94	422	4472	0.01	2.510	0.0030	0.3954
	DMSO	358	2.89	425	4404	0.01	2.427	0.0027	0.4093
	ACN	352	3.38	419	4543	0.01	2.208	0.0027	0.4502
	i-PrOH	352	4.01	421	4656	0.02	1.421	0.0124	0.6913
	EtOH	352	4.35	422	4712	0.01	1.306	0.0079	0.7578
	MeOH	351	3.50	434	5449	-	1.402	0.0022	0.7110
	Water	354	1.61	451	6076	-	2.938	0.0014	0.3389

Table 4.

Compound		y_o	a	b	c	r
1	ν_{abs}	28343.87 ± 97.85	236.88 ± 46.71	-291.13 ± 134.38	-583.29 ± 94.26	0.95
	ν_{flu}	24490.83 ± 209.84	-854.16 ± 100.17	323.76 ± 288.19	-1152.81 ± 202.14	0.98
2	ν_{abs}	28282.92 ± 108.11	219.05 ± 51.61	-282.50 ± 148.47	-558.99 ± 104.14	0.94
	ν_{flu}	24550.46 ± 197.64	-890.46 ± 94.35	342.92 ± 271.44	-1226.91 ± 190.39	0.98
3	ν_{abs}	28249.29 ± 121.56	198.00 ± 58.03	-240.55 ± 166.95	-522.27 ± 117.09	0.91
	ν_{flu}	24474.70 ± 186.74	-850.14 ± 89.15	338.22 ± 256.46	-1168.91 ± 179.88	0.98
4	ν_{abs}	28482.16 ± 91.30	237.04 ± 43.59	-406.77 ± 125.39	-640.22 ± 87.95	0.96
	ν_{flu}	24550.46 ± 197.64	-890.46 ± 94.35	342.92 ± 271.44	-1226.91 ± 190.39	0.98
5	ν_{abs}	28425.69 ± 75.99	213.18 ± 36.28	-344.56 ± 104.37	-586.11 ± 73.21	0.97
	ν_{flu}	24495.59 ± 208.12	-827.79 ± 99.35	354.70 ± 285.83	-1186.46 ± 200.48	0.98
6	ν_{abs}	28445.07 ± 103.60	182.83 ± 49.45	-336.42 ± 142.28	-581.06 ± 99.79	0.94
	ν_{flu}	24495.50 ± 201.11	-837.53 ± 96.01	387.75 ± 276.21	-1184.81 ± 193.73	0.98
7	ν_{abs}	28801.11 ± 96.83	197.69 ± 46.23	-311.86 ± 132.99	-564.77 ± 93.28	0.95
	ν_{flu}	24364.45 ± 288.10	-818.22 ± 137.53	791.62 ± 395.67	-1421.15 ± 277.52	0.96

Table 5.

Compound		y_o	a	b	c	d	r
1	ν_{abs}	29692.84 ± 99.34	-14.30 ± 32.86	-5.90 ± 42.87	-2386.47 ± 132.04	-211.34 ± 40.77	0.99
	ν_{flu}	25353.25 ± 195.25	-1563.43 ± 64.58	-84.83 ± 84.27	-1761.69 ± 259.52	-170.35 ± 80.13	0.99
2	ν_{abs}	29631.96 ± 129.31	-68.22 ± 42.77	-36.44 ± 55.81	-2420.61 ± 171.87	-127.24 ± 53.07	0.99
	ν_{flu}	25469.49 ± 199.03	-1621.81 ± 65.83	-67.33 ± 85.90	-1882.71 ± 264.55	-196.10 ± 81.68	0.99
3	ν_{abs}	29548.39 ± 136.66	-85.47 ± 45.20	-28.98 ± 58.98	-2336.31 ± 181.65	-85.23 ± 56.08	0.99
	ν_{flu}	25352.20 ± 262.20	-1539.77 ± 86.72	-51.37 ± 113.16	-1802.16 ± 348.50	-184.24 ± 107.60	0.99
4	ν_{abs}	29942.32 ± 135.11	-68.82 ± 44.69	-87.80 ± 58.31	-2575.13 ± 179.58	-251.42 ± 55.44	0.99
	ν_{flu}	25469.49 ± 199.03	-1621.81 ± 65.83	-67.33 ±85.90	-1882.71 ± 264.55	-196.10 ± 81.68	0.99
5	ν_{abs}	29735.60 ± 121.90	-60.30 ± 40.32	-59.63 ± 52.61	-2324.27 ± 162.02	-220.76 ± 50.02	0.99
	ν_{flu}	25416.57 ± 170.83	-1532.71 ± 56.50	-37.84 ± 73.73	-1882.47 ± 227.06	-171.79 ± 70.10	0.99
6	ν_{abs}	29767.07 ± 126.74	-104.73 ± 41.92	-70.52 ± 54.70	-2350.10 ± 168.46	-197.39 ± 52.01	0.99
	ν_{flu}	25400.60 ± 187.58	-1535.99 ± 62.04	-13.18 ± 80.96	-1874.61 ± 249.33	-152.53 ± 76.98	0.99
7	ν_{abs}	30096.31 ± 143.73	-79.46 ± 47.54	-54.03 ± 62.03	-2302.27 ± 191.04	-184.35 ± 58.98	0.99
	ν_{flu}	25342.72 ± 532.79	-1434.25 ± 176.22	363.01 ± 229.94	-2020.41 ± 708.16	-283.51 ± 218.64	0.98

SUPPLEMENTARY MATERIAL

Solvent and Substituent Effect on the Photophysical Properties of Pyrazoline Derivatives: A Spectroscopic Study

Ebru Bozkurt[a*], Halise Inci Gul[b], Ebru Mete[c]

[a]*Program of Occupational Health and Safety, Erzurum Vocational Training School, Ataturk University, 25240 Erzurum, Turkey*

[b]*Department of Pharmaceutical Chemistry, Faculty of Pharmacy, Ataturk University, 25240 Erzurum, Turkey*

[c]*Department of Chemistry, Faculty of Science, Ataturk University, TR-25240 Erzurum, Turkey*

** Tel: +90(442)231 2667; Fax #: +90(442)231 2503*

e-mail: ebrubozkurt@atauni.edu.tr (Ebru Bozkurt)

4-[3-(4-Hydroxyphenyl)-5-phenyl-4,5-dihydro-pyrazol-1-yl]benzenesulfonamide (1)

M.p. 208–210 ^{0}C. Yield: 47%. ^{1}H NMR (400 MHz, CD3OD, ppm) d ¼ 7.65 (d, 2H, J ¼ 8.8 Hz), 7.64 (d, 2H, J ¼ 9.0 Hz), 7.36–7.24 (m, 5H), 7.08 (d, 2H, J ¼ 9.0 Hz), 6.84 (d, 2H, J ¼ 8.8 Hz), 5.43 (dd, 1H, J ¼ 12.0, 5.7 Hz), 3.92 (dd, 1H, J ¼ 17.4, 12.0 Hz), 3.13 (dd, 1H, J ¼ 17.4, 5.7 Hz); ^{13}C NMR (100 MHz, CD_3OD, ppm) d ¼ 160.2, 151.5, 148.7, 143.5, 132.8, 130.3, 128.9, 128.8, 128.5, 126.9, 125.0, 116.5, 113.3, 64.5, 44.7; HRMS (ESI-MS): calcd. for $C_{21}H_{20}N_3O_3S$ $[M + H]^+$ 394.1225; found 394.1217.

4-[3-(4-Hydroxyphenyl)-5-p-tolyl-4,5-dihydro-pyrazol-1-yl]benzenesulfonamide (2)

M.p. 163–164 ^{0}C. Yield: 75%. ^{1}H NMR (400 MHz, CD3OD, ppm) d ¼ 7.62 (d, 2H, J ¼ 8.8 Hz), 7.61 (d, 2H, J ¼ 9.1 Hz), 7.20–7.10 (m, 4H), 7.05 (d, 2H, J¼8.8 Hz), 6.82 (d, 2H, J¼8.8 Hz), 5.37 (dd, 1H, J¼12.1, 5.5 Hz), 3.87 (dd, 1H, J¼17.4, 12.1 Hz), 3.08 (dd, 1H,

J¼17.4, 5.5 Hz), 2.28 (s, 3H, –CH3); ^{13}C NMR (100 MHz, CD_3OD, ppm) d¼159.0, 150.3, 147.5, 139.2, 137.4, 131.5, 129.6, 127.7, 127.3, 125.6, 123.8, 115.3, 112.1, 63.1, 43.5, 19.9; HRMS (ESI-MS): calcd. for $C_{22}H_{22}N_3O_3S$ $[M + H]^+$ 408.1382; found 408.1367.

4-[3-(4-Hydroxyphenyl)-5-(4-methoxyphenyl)-4,5-dihydropyrazol-1-yl]benzenesulfonamide (3)

M.p. 176–178 ^{0}C. Yield: %23. ^{1}H NMR (400 MHz, CD3OD, ppm) d¼7.62 (d, 2H, J¼8.8 Hz), 7.61 (d, 2H, J¼8.8 Hz), 7.16 (d, 2H, J¼8.8 Hz), 7.06 (d, 2H, J¼8.8 Hz), 6.86 (d, 2H, J¼8.8 Hz), 6.82 (d, 2H, J¼8.8 Hz), 5.36 (dd, 1H, J¼12.1, 5.5 Hz), 3.86 (dd, 1H, J¼17.2, 12.1 Hz), 3.74 (s, 3H, -OCH3), 3.09 (dd, 1H, J¼17.2, 5.5 Hz); ^{13}C NMR (100 MHz, CD_3OD, ppm) d¼159.5, 159.0, 150.3, 147.6, 134.1, 131.4, 127.7, 127.2, 126.9, 123.9, 115.3, 114.4, 112.1, 62.9, 54.5, 43.5; HRMS (ESI-MS): calcd. for $C_{22}H_{22}N_3O_4S$ $[M + H]^+$ 424.1331; found 424.1312.

4-[5-(4-Bromophenyl)-3-(4-hydroxyphenyl)-4,5-dihydro-pyrazol-1-yl]benzenesulfonamide (4)

M.p. 174–175 ^{0}C. Yield: 38%. ^{1}H NMR (400 MHz, CD3OD, ppm) d¼7.64 (d, 2H, J¼8.8 Hz), 7.63 (d, 2H, J¼8.8 Hz), 7.48 (d, 2H, J¼8.4 Hz), 7.19 (d, 2H, J¼8.4 Hz), 7.05 (d, 2H, J¼9.1 Hz), 6.82 (d2H, J¼8.8 Hz), 5.42 (dd, 1H, J¼12.1, 5.5 Hz), 3.91 (dd, 1H, J¼17.6, 12.1 Hz), 3.12 (dd, 1H, J¼17.6, 5.5 Hz); ^{13}C NMR (100 MHz, CD_3OD, ppm) d¼159.1, 150.3, 147.3, 141.5, 132.1, 131.9, 127.8, 127.7, 127.4, 123.6, 121.2, 115.3, 112.1, 62.7, 43.3; HRMS (ESI-MS): calcd. for $C_{21}H_{19}BrN_3O_3S$ $[M + H]^+$ 472.0330; found 472.0317.

4-[5-(4-Chlorophenyl)-3-(4-hydroxyphenyl)-4,5-dihydro-pyrazol-1-yl]benzenesulfonamide (5)

M.p. 152–154 ^{0}C. Yield: 62%. ^{1}H NMR (400 MHz, CD3OD, ppm) d¼7.64 (d, 2H, J¼8.8 Hz), 7.63 (d, 2H, J¼8.8 Hz), 7.32 (d, 2H, J¼8.4 Hz), 7.26 (d, 2H, J¼8.4 Hz), 7.05 (d, 2H, J¼9.2 Hz), 6.82 (d, 2H, J¼8.8 Hz), 5.45 (dd, 1H, J¼12.1, 5.5 Hz), 3.91 (dd, 1H, J¼17.2, 12.1 Hz), 3.12 (dd, 1H, J¼17.2, 5.5 Hz); ^{13}C NMR (100 MHz, CD_3OD, ppm) d¼159.1, 150.3, 147.3, 141.0, 133.3, 131.9, 129.1, 127.8, 127.5, 127.4, 123.6, 115.3, 112.1, 62.6, 43.3; HRMS (ESI-MS): calcd. for $C_{21}H_{19}C_lN_3O_3S$ $[M + H]^+$ 428.0836; found 428.0824.

4-[5-(4-Fluorophenyl)-3-(4-hydroxyphenyl)-4,5-dihydro-pyrazol-1-yl]benzenesulfonamide (6)

M.p. 243–244 ^{0}C. Yield: 72%. ^{1}H NMR (400 MHz, CD3OD, ppm) d¼7.63 (d, 4H, J¼8.8 Hz), 7.30–7.26 (m, 2H), 7.07–7.03 (m, 4H), 6.82 (d, 2H, J¼8.8 Hz), 5.45 (dd, 1H, J¼12.1, 5.5 Hz), 3.90 (dd, 1H, J¼17.6, 12.1 Hz), 3.11 (dd, 1H, J¼17.6, 5.5 Hz); ^{13}C NMR (100 MHz, CD_3OD, ppm) d¼159.1, 150.3, 147.4, 138.2, 131.8, 127.8, 127.7, 127.3, 123.7, 115.8, 115.6, 115.3, 112.1, 62.6, 43.5; HRMS (ESI-MS): calcd. for $C_{21}H_{19}FN_3O_3S$ $[M + H]^+$ 412.1131; found 412.1115.

4-[3-(4-Hydroxyphenyl)-5-(4-nitrophenyl)-4,5-dihydro-pyrazol-1-yl]benzenesulfonamide (7)

M.p. 173–176 ^{0}C. Yield: 61%. ^{1}H NMR (400 MHz, CD3OD, ppm) d¼8.20 (d, 2H, J¼8.8 Hz), 7.65 (d, 2H, J¼9.2 Hz), 7.64 (d, 2H, J¼8.8 Hz), 7.51 (d, 2H, J¼8.8 Hz), 7.05 (d, 2H, J¼9.2 Hz), 6.82 (d, 2H, J¼8.8 Hz), 5.60 (dd, 1H, J¼12.1, 5.5 Hz), 3.97 (dd, 1H, J¼17.6, 12.1 Hz), 3.17 (dd, 1H, J¼17.6, 5.5 Hz); ^{13}C NMR (100 MHz, CD_3OD, ppm) d¼159.2, 150.3, 149.5, 147.7, 147.2, 132.3, 127.9, 127.5, 127.1, 124.2, 123.4, 115.4, 112.1, 62.6, 43.1; HRMS (ESI-MS): calcd. for $C_{21}H_{18}N_4O_5S$ $[M + H]^+$ 437.0920; found 437.0931.

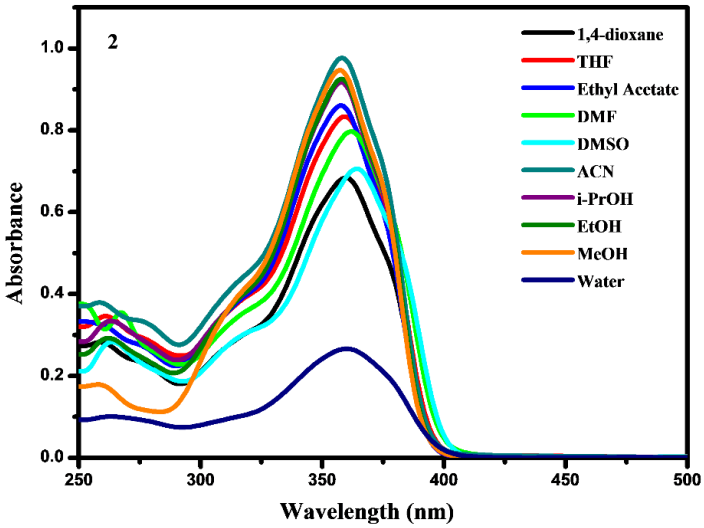

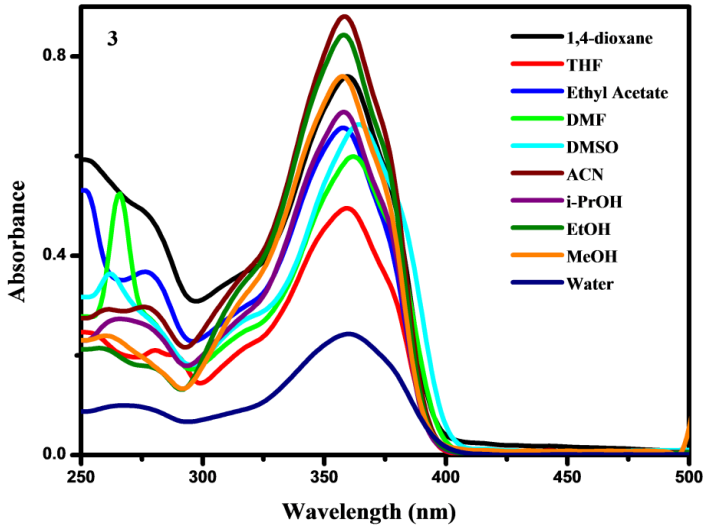

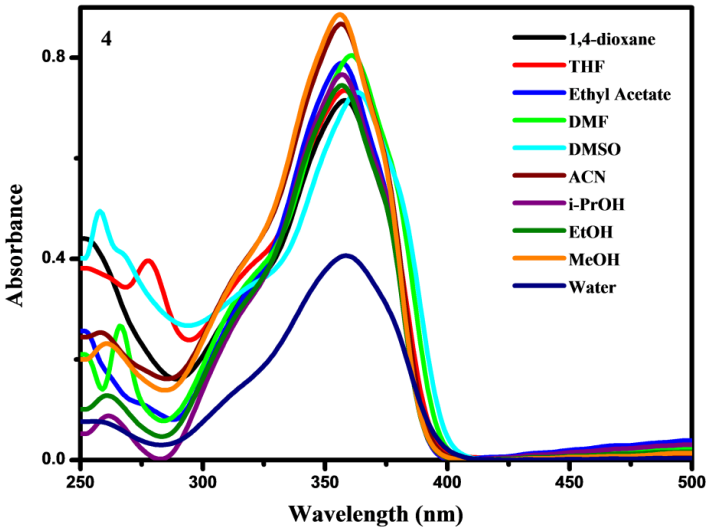

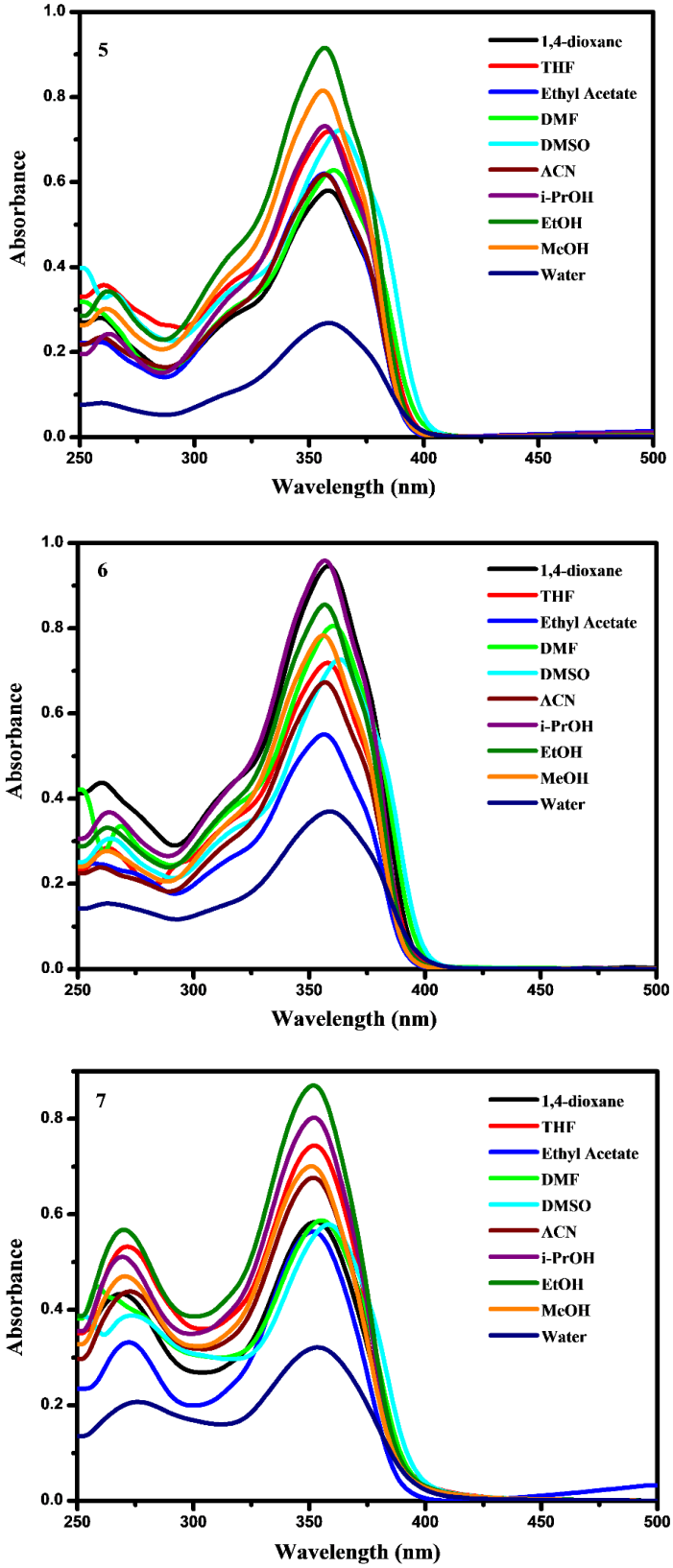

Fig. S1. The absorption spectra of pyrazoline derivatives **2-7** in different solvents.

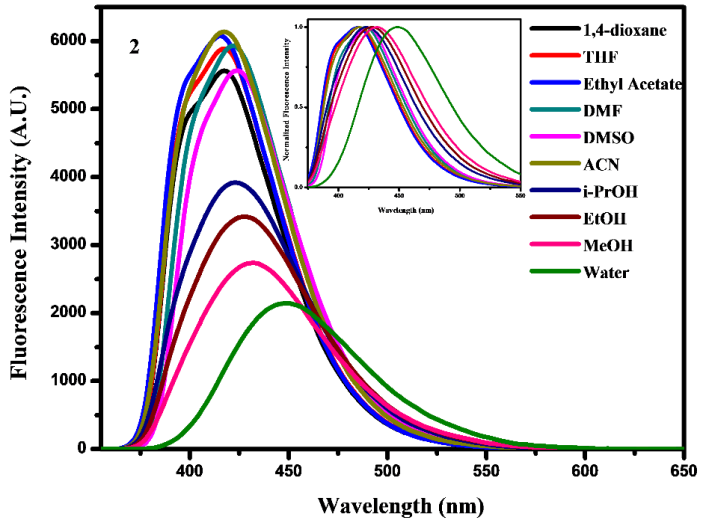

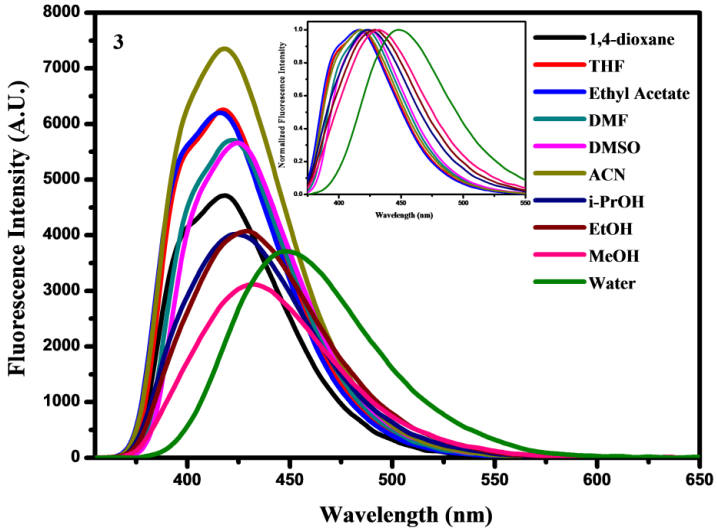

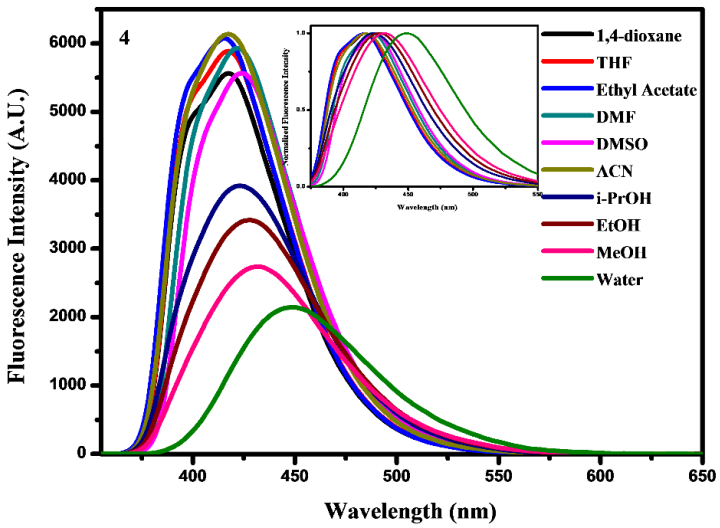

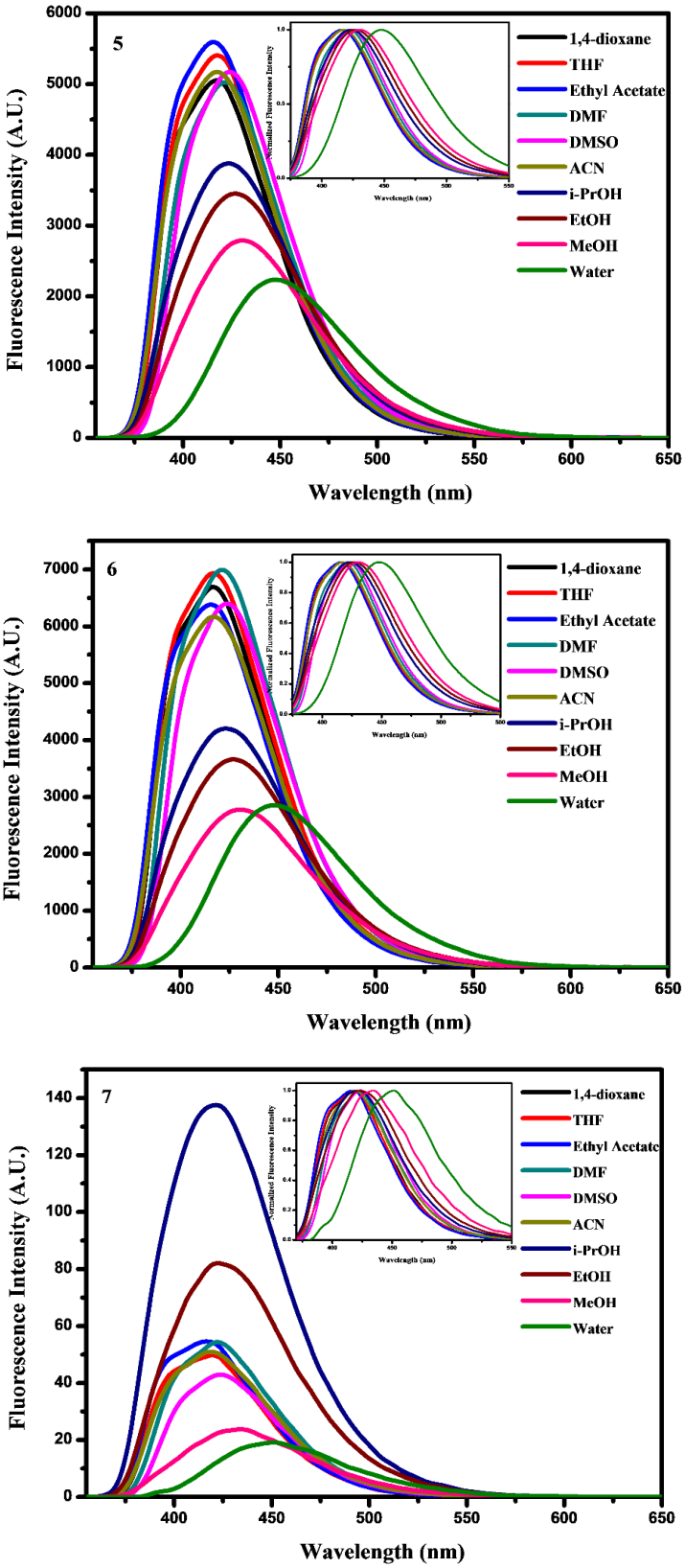

Fig. S2. The fluorescence spectra of pyrazoline derivatives **2-7** in different solvents. Inset: Normalized fluorescence spectra of pyrazoline derivatives in different solvents.